J. COMBIN. MATH. COMBIN. COMPUT. 127a (2025) 7119--7134

Journal of Combinatorial Mathematics
and Combinatorial Computing
www.combinatorialpress.com/jcmcc

Study on the Possibility of Combining Abrasive Painting Technique with Algorithmically Generated Color Distribution Methods in Lacquer Painting Creation

Meijian Wu[1,✉]

[1] *Academy of Fine Arts, Zhaoqing University, Zhaoqing, Guangdong, 526061, China*

ABSTRACT

As a conventional technique in lacquer painting, the abrasion painting technique is widely used in the creation of modern lacquer painting. In order to promote the digital innovation of the abrasion painting technique in the creation of lacquer paintings, a fusion scheme of the abrasion painting technique and color distribution in the creation of lacquer paintings is formulated. According to the relationship between color and gray scale, the color mapping of image coloring algorithm is proposed under the framework of energy optimization algorithm to realize algorithm-driven lacquer painting color generation. In addition, with the technical support of the renderer, the color distribution of lacquer paintings is integrated with the milling technique according to the principle of texture mapping. With the help of evaluation indexes and experimental platforms, we simulate and analyze the techniques and colors in lacquer painting. In the color generation of lacquer paintings, the indicators of this paper's method are 34.09, 0.964, 0.025 and 4.28 in order, which verifies the application effect of this paper's method in the color generation of lacquer paintings. In addition, the speed of this paper's rendering method (42-86FPS), fully meets the requirements of real-time drawing, this method better promotes the fusion of grinding and painting techniques and color distribution in the creation of lacquer paintings, which is of great significance to the digital dissemination of traditional culture of non-heritage.

Keywords: abrasive painting techniques, lacquer painting, image coloring algorithms, renderers

1. Introduction

Throughout the historical process of the development of lacquer painting, lacquer painting has its unique cultural value and historical significance, the lacquer art was born because of the ware, after a long history of development, detached from the artifacts in the twentieth century in the twentieth and thirtieth centuries gradually formed [1]. The real uniqueness of lacquer painting lies firstly in the

✉ Corresponding author.
E-mail address: zquart@163.com (M. Wu).
Received 03 March 2024; Revised 20 April 2024; Accepted 10 November 2024; Published Online 15 April 2025.
DOI: 10.61091/jcmcc127a-396
© 2025 The Author(s). Published by Combinatorial Press. This is an open access article under the CC BY license (https://creativecommons.org/licenses/by/4.0/).

difference of its applied materials, and secondly in the uniqueness of its techniques. The main techniques of lacquer painting include powdering, inlaying, carving, stacking, grinding and painting, etc. Compared with other painting techniques, the grinding and painting technique has a unique form of expression, which is mainly embodied in its unique creative behavior, painting through grinding, both in the language of color and material language has its special visual experience, and the behavior of grinding in grinding is a kind of behavioral expression of writing [2-4]. As one of the most basic techniques in lacquer painting, the grinding technique has been continuously developed along with the development of lacquer art. From the initial production of the base tire to the final overall grinding and polishing, grinding and painting technique has always been throughout the entire lacquer art creation, tracing back to the roots can be found, grinding and painting technique was first seen in the Tang Dynasty gold and silver flat off the feathered man flying phoenix lacquer backed bronze mirror, which is engraved with silver and gold into a skeleton pattern and then pasted on the lacquer coated and ground, and then applied in all subsequent periods [5-6]. It can be seen that the grinding and painting technique has its unique aesthetic value and significance for the creation of lacquer paintings.

With the development of modern technology, algorithmically generated artistic expressions are becoming more and more popular. Algorithmic generation is the process of generating artworks through computer processing based on specific algorithms and rules [7]. This method is capable of generating works of art with uniqueness, complexity and creativity. Algorithms can be used to generate various forms of artworks such as images, music, animation, etc. In this field, artists use various algorithms and computer programs to generate visual, musical, literary and other forms of artworks [8-11]. These algorithms can be based on mathematical models, based on artificial intelligence, based on the laws of nature, etc., and through these algorithms, artists can create unique and creative works [12]. This has become an excellent technique in the field of art creation, especially in the creation of paintings, where painting images are represented digitally and advanced algorithms are used to generate the target painting map [13]. Algorithmic generation will become an inevitable trend in the field of painting creation, and the traditional painting techniques bring together a number of advantages, if the combination of the two for the creation of art, it must be a new opportunity for art creation, such as the painting works of strong color contrast and realistic effect of good [14].

Taking the characteristics of the grinding painting technique as the entry point of this research, the aesthetic performance of the grinding painting technique in the color language of lacquer paintings is elaborated in detail, and a preliminary theoretical analysis of the relationship between the grinding technique and color is made to lay a theoretical foundation for the following research work. In between the relationship between color and grayscale, the image coloring algorithm is used to complete the color generation part of the lacquer painting creation process. Collective renderer, texture mapping, to promote the integration of color distribution and grinding painting techniques, and verification analysis of the above research program. Based on the research results, the promotion effect of this paper's method on the digital dissemination of non-heritage traditional culture is summarized, and the corresponding outlook is also proposed for the research deficiency of this paper.

2. Abrasion techniques in the creation of lacquer paintings

2.1. Characteristics of the milling technique

2.1.1. Sense of reality. The concept of “reality and emptiness” is an important category in ancient philosophy, as mentioned by Laozi in the Tao Te Ching: “The great sound has no sound, and the great image has no form” [15-16]. It is meant to be a description related to music, explaining that the best music is the absence of sound, and the best image is the absence of image. The intention is to express a natural beauty rather than man-made beauty. This is exactly the case with the presentation of the sense of reality in mill painting, although the sense of reality is reflected in many paintings, for example, the visual expression of the distant mountains and rocks and clouds in Chinese painting presents a sense of beauty of reality and emptiness. For example, in Chinese painting, the visual representation of distant mountains and rocks as well as clouds and mist presents a sense of emptiness and reality. Or in oil painting, the impressionist painting method uses blurred scenes with subtle color changes to present the beauty of emptiness and reality in the picture. But in lacquer painting is very different, the sense of reality in lacquer painting comes from the characteristics of lacquer and other materials on the one hand, and on the other hand, it relies on the technique of grinding and painting, through the layers of color stacking and texture of the pre-embedded, and then use the grinding stone for grinding to show that different strength will have different visual effects. The whole process is a kind of embodiment from "something" to "nothing", and the change of reality and emptiness presented through the grinding painting cannot be imitated by other paintings. The visual effect, both in terms of color language and material language, reveals the beauty of a deep and distant change.

2.1.2. Hierarchy. The famous scholar Terry Possumal once referred to the "iterative method". It refers to the process of creating complexity through the repetition of simple behavioral actions, i.e., through subjective awareness, the spatial traces left intentionally or unintentionally in the lacquer layer are hidden in the organic form of the lacquer layer, which can only be perceived under ambient light. On this basis, if we continue to repeat the operation over and over again, countless complex visual forms will emerge along with the grinding and painting [17-18]. This is exactly how the layered sense of mill painting technique is reflected, presenting a layered space that is as unpredictable as the contour lines of a map. Although other paintings also present complex layered space in the process of creation, especially in comprehensive paintings where the visual presentation of materials has a strong tension, there is a difference in essence. The layers of other paintings are presented through continuous stacking, which is a process of "addition", while the grinding and painting in lacquer painting is a process of "subtraction". The "iterative" traces are visualized by stacking the lacquer paintings in the early stage, and then reducing them by using the abrasive painting technique. The abrasive painting technique makes the potential spatial layers in the creation process of lacquer paintings perfectly presented.

2.2. Aesthetic Expression of Abrasive Painting Technique in Color Language

2.2.1. Rich and subtle beauty in color language. Abrasive painting technique paints by "grinding", applying color lacquer on the lacquer board through the pre-built texture and then grinding to paint, presenting rich and subtle color visual effects in the process of grinding. Its richness comes from the different degrees of grinding of the color layers of a single material through the grinding process, which presents unpredictable visual effects. Its subtlety comes from the deep and timeless aesthetic feeling brought about by grinding and painting. Such as through the bottom layer sprinkled with a thicker mesh of silver powder and then cover transparent lacquer and then polished on top of the push light, the final effect is the bottom layer of silver powder grinding out, can be seen in the figure on the green surface layer of lacquer through the hidden silver powder luster and lacquer layer reflecting the visual aesthetic sense of subtlety. Such as by laying aluminum powder on the good paint layer, and then cover transparent lacquer for polishing, which aluminum powder cover transparent presents a warm golden luster. In the picture for the original single color to add a complementary color relationship, and through the grinding of the color relationship with the black part of the painting directly next to the obvious difference. Firstly, the color line is not so hard and is more soft and harmonious, and secondly, the color changes are more subtle and dynamic. By applying the transparent foil cover and then painting and polishing, it can be clearly seen in the picture that the area and luster of the gold foil presented by different strengths of the degree of grinding and painting are different, and the single color of the gold foil will be presented by grinding and painting with different color levels and rich visual effects.

2.2.2. Misty and mysterious color levels. In the process of lacquer painting, the layers of lacquer are painted, and then the "reduction" is carried out by grinding and painting techniques so that the lacquer layer buried underneath can be revealed, and the painting is carried out by grinding, and then polished and wiped with lacquer according to the effect of the picture and the need to polish the picture. The whole process is an action from "plus" to "minus", through grinding and painting to make a single color layer presents multi-layered haze and the surface of the surface of the polishing presents a sense of mirror and gives the picture a hint of mystery. The picture is painted by spreading powder and outlining in the early stage, then painting and coloring in layers by superimposing techniques, and finally polished by subtracting with the technique of grinding and painting. The whole picture is in blue, but the yellow-green color underneath the ambush is revealed through grinding and painting, and intertwined with the blue color on the surface, forming a subtle color change and bringing the picture a kind of hazy and mysterious aesthetic feeling.

3. Integration of Color Distribution and Abrasive Painting Techniques

3.1. Image coloring algorithm

3.1.1. Color and Gray Scale Relationships. Our aim is to verify whether the color and gray scale relationships within each segmented region satisfy a one-dimensional segmented linear model. Inspired by the color line algorithm of Ido et al. we use a segmented fitting algorithm as follows:

1) For each labeled region in the image, find its principal direction using the PCA algorithm.

2) Map all points in the region to the principal direction to get the order of the points.

3) Cluster the points in every Δ interval from the first to the last point in the principal direction and find the clustering center C_k for each class k_{th}.

4) Connect each cluster center to obtain a continuous line segment.

5) Calculate the error after fitting the line segments.

The above algorithm is designed based on the color line fitting algorithm. In the color line algorithm, multiple color lines are fitted simultaneously to get. Our algorithm, on the other hand, needs to fit only one one-dimensional line, which has a relatively small uncertainty and a simpler algorithm. This algorithm provides a way to roughly estimate the validity of the model. In order to analyze the model fitting error, we use the length ratio (L Ratio) measure commonly used in error analysis, which is expressed as follows:

$$LRatio = error / \sum_{k=1,\dots N-1} \| C_{k+1} - C_k \| \tag{1}$$

where error is the fitting error, in this case the average distance of the data points from the fitted line segment. $\| C_{k+1} - C_k \|$ is the length of the k nd line segment. The value of length ratio estimates the coarseness of the clustering cluster. For this type of one-dimensional streaming, the finer the cluster cluster, the better the fit.

For each marked region in each image of the Berkeley image library, we calculated the LRatio values and analyzed them. Figure 1 shows the comparative analysis of LRatio values. It can be seen that the LRatio of most of the regions is in the range of 0 to 0.15. Figure 2 shows the distribution of LRatio in each image. It can be seen that 75% or even 100% of the regions in most of the images in the image library have LRatio less than 0.06. The analysis shows that most of the regions in the natural images have colors that conform better to our 1-dimensional segmented linear model.

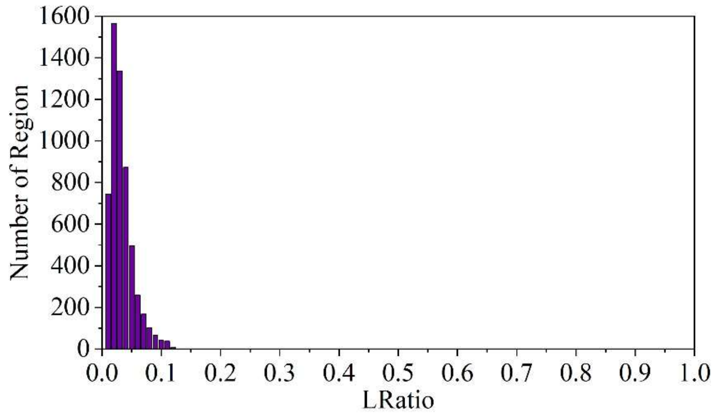

Fig. 1. Comparative analysis of LRatio value

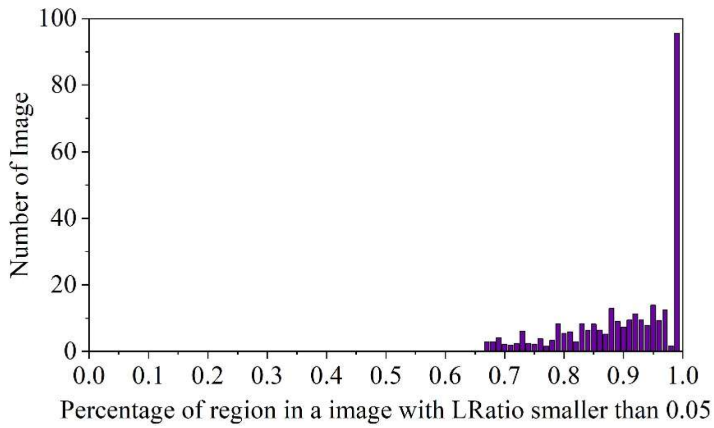

Fig. 2. The distribution of LRatio in each image

3.1.2. Energy optimization algorithm framework. By analyzing and experimenting with the properties of textured and smoothed regions in grayscale images we found that smoothed pixel locations and high contrast pixel locations possess complementary properties:

1) High-contrast regions have more prominent texture properties and make fewer errors in clustering.

2) The color of a pixel in a smoothed region can be determined by its surrounding pixels.

Inspired by the above properties we design a unified energy framework that integrates texture similarity and gray-scale continuity. Here, we introduce a key guiding quantity, the smoothness parameter $\lambda(p)$. In our energy framework, the smoothness parameter guides the proportion of the two items, texture similarity and grayscale continuity, in the energy. When the smoothness parameter is large, we believe more in grayscale continuity, while when the smoothness parameter is small, we believe more in texture similarity. In this paper, we use a Gaussian smoothed Canny edge map for the smoothness parameter. We denote the similarity of each pixel p pair of markers as $L(C;p)$, where the vector $C=[C_1,C_2,\dots,C_N]^T$, represents all the markers. Our energy equation is:

$$E=\sum_{p\in img}(\lambda(p)E_1+(1-\lambda(p))E_2) \tag{2}$$

where E_1 is the texture energy term and E_2 is the spatial energy term, which are as follows:

$$E_1=\sum_{q\in\Omega_t(p)} w^t_{pq}\,\|L(C;p)-L(C;q)\| \tag{3}$$

$$E_2 = \sum_{q \in \Omega_*(p)} w^s_{pq} \| L(C;p) - L(C;q) \| \tag{4}$$

The hard constraints for the energy optimization are $L(C;p) = [0,\ldots,1_k,\ldots 0]^T, p \in stroke_k$, where $stroke_k$ is an input line that possesses the color of marker C_k. In the following sections, we describe the definition of the neighborhood $\Omega_t(p)$ in the texture term and the neighborhood $\Omega_s(p)$ in the spatial term.

3.1.3. Texture field. Each point of pixel p that is similar in texture properties we call it the texture neighborhood of this pixel, denoted as $\Omega_t(p)$. In order to obtain the pixel's texture neighborhood relationship, we first cluster the small squares around the pixel using a preprocessing texture analysis step. In this step, we cluster the small squares around the image based on its appearance. The image contains a large number of pixels, and clustering the appearance of the perimeter of each pixel is a very time-consuming operation. Also, based on the texture properties we discussed at the beginning of this chapter, here we are only concerned with those high contrast points. Those small square regions around the pixels that become edge points after Canny edge detection are involved in clustering, using the k-means clustering algorithm with SSD distance for clustering. The number of clusters was set to a large value (we set it to 500), thus ensuring that the small squares inside each class are very similar. After clustering, the categorization of where the small squares are located in the image within each class, for those small squares that are sparsely located in space and are not contiguous, we further classify them into different classes.

3.1.4. Iterative energy optimization. The energy is optimized by diffusing L iteratively through the texture and spatial neighborhood thus. The sending equation is as follows:

$$L^0(C;p) = \begin{cases} (0,\ldots,1_k,\ldots,0)^T & p \in stroke_k \\ (\frac{1}{N},\ldots,\frac{1}{N},\ldots,\frac{1}{N})^T & otherwise \end{cases} \tag{5}$$

$$\begin{aligned} L^{n+1}(C;p) = \lambda(p) \sum_{q \in \Omega_t(p)} w^t_{pq} L^n(C;q) \\ +(1-\lambda(p)) \sum_{q \in \Omega_s(p)} w^s_{pq} L^n(C;q) \end{aligned} \tag{6}$$

Since $\Omega_s(p)$ is defined as the 8-neighborhood of pixel p, optimizing the whole image to get the color markers for each pixel is very slow, and for a 400*400 image it will probably take about 100 iterative loops and close to 2 minutes to complete the optimization. In order to speed up, we over-segment the image first to get the super-pixels of the image, and then optimize on the super-pixel neighborhood. It is possible to speed up the 400*400 size image by almost 30 times, and for this image, L was stabilized in only 3 iteration steps.

3.1.5. Color Mapping. Color labeling yields segmentation results for almost homogeneous material regions, meeting the prerequisites for segmented linear models. Next, we introduce the unique coloring method, color mapping, which is different from the previous algorithms in this paper.

The points in the region selected by the user are the anchors for the color linear interpolation, denoted as $(I_k, C_k), k = 1 \ldots N$. Where I_k, C_k are the grayscale values of the k rd anchor point and the C_bC_r two-dimensional color vectors, respectively, and $I_k, k = 1 \ldots N$ are not equal to each other, the user's specification will be invalidated if the user specifies a grayscale that is equal to an existing I_k one. The color of all points in the region with a grayscale of I is calculated as follows:

$$C(I)=\begin{cases} C_{k-1}\dfrac{I-I_{k-1}}{I_k-I_{k-1}}+C_k\dfrac{I_k-I}{I_k-I_{k-1}} & I\in[I_{k-1},I_k] \\ C_N & I>\max(I_k) \\ C_0 & I<\min(I_k) \end{cases} \tag{7}$$

where $k\in[1,..N]$. The color of the entire image is obtained by color mapping each region. It is worth noting that after color mapping, the final colors of the different regions are not rigidly spliced together. For the colors of different adjacent regions, we use a gradient transition process. In a wide band in the neighborhood of adjacent zones, we iterate the energy so as to get a weight per pixel for each marker. The color of this region is then obtained by superimposing this weight.

3.2. Renderer-based color distribution and fusion of mill painting techniques

There are many kinds of abrasive painting techniques in lacquer painting, and there are big differences in expression between various abrasive painting techniques, while painters are more spontaneous in painting with this technique, and it is impossible to propose an algorithm for each abrasive painting technique. Therefore, in this paper, the texture map is generated by mixing and connecting multiple color distribution regular textures of lacquer painting techniques, and then based on the two-step texture mapping method to realize the integration of color distribution and lacquer painting techniques.

3.2.1. Creation of color-mapped texture maps for abrasive painting techniques. A collection of regularized mill mapping techniques has been obtained after mill mapping technique characterization. $S_k^{textawe}=\{s_i\mid i=1,2,3,\cdots\}$ Now multiple textures are linearly blended and connected to form a large mapped texture map. First, the number of interpolated textures is determined N, and the average values of the H information for the abrasion technique textures A and B are μ_A and μ_B, then $N=|\mu_A-\mu_B|/k$. A factor of k is used to control the degree of jumps in the transitions between abrasion technique textures, where the larger k is, the smaller N is, and the greater the degree of variation between the abrasion techniques. $k=5$ is used in the paper, and then the interpolated image between A and B is $I_{berween}$:

$$I_{berween}=\alpha\cdot A+(1-\alpha)\cdot B,\alpha=1,\frac{N-1}{N},\frac{N-2}{N},\cdots,0 \tag{8}$$

Obviously, when $\alpha=1$, the image A is taken, and when $\alpha=0$, the image B.

3.2.2. S-O two-step texture mapping. In order to optimize the rendering results, the S-O two-step texture mapping method is used to draw the model by the method. The basic idea is not to directly texture map the surface of the 3D model, but to introduce an intermediate transition surface, and decompose the mapping process into a two-step operation: the first step is the mapping from the textured plane to the transition surface, i.e., $T(u,v)\rightarrow S(x',y',z')$, which becomes S-mapping. The second step is the mapping from the transition surface to the surface of the 3D model, i.e., $S(x',y',z')\rightarrow O(x,y,z)$, which is called O-mapping.The transition surfaces in S-mapping are usually simple 3D surfaces, such as spheres, cylinders, and cubes.The four forms of O-mapping are shown in Fig. 3.

There can be 12 combinations of S-mapping and O-mapping, in this paper, we take the sphere as the transition surface of S-mapping and modify the third O-mapping method to be drawn by the milling technique.

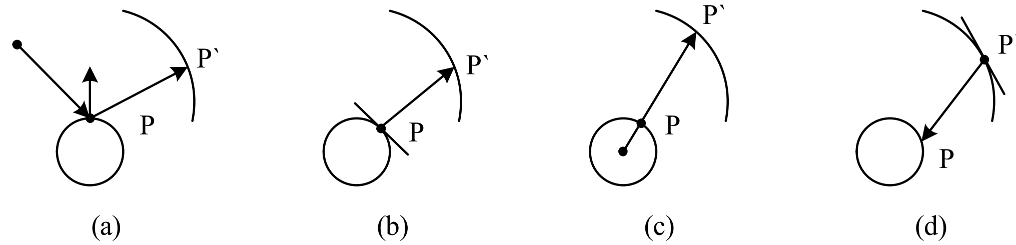

Fig. 3. Four modes of O mapping

1) S-mapping: The transition surface sphere is divided into two parts symmetric along xy plane, and the mapping algorithm with area equipartition constraints is utilized to map the texture to the two parts symmetric to the sphere respectively. The mapping of s on the sphere is shown in Fig. 4. Given a two-dimensional texture coordinate system uv, the center of the texture plane coincides with the origin of the coordinate system, and any point $P(u,v)$ can be expressed in polar coordinates (ρ,α). Given a three-dimensional coordinate system xyz, the center of the spherical plane of radius R coincides with the origin, and any point $Q(x,y,z)$ of the spherical plane can be expressed in spherical coordinates as (R,θ,ϕ). Due to symmetry, the spherical plane can be divided into upper and lower hemispheres by the xy-plane, and the method of mapping the two hemispheres is the same, and only the algorithm for mapping the texture on the upper hemisphere is discussed here.

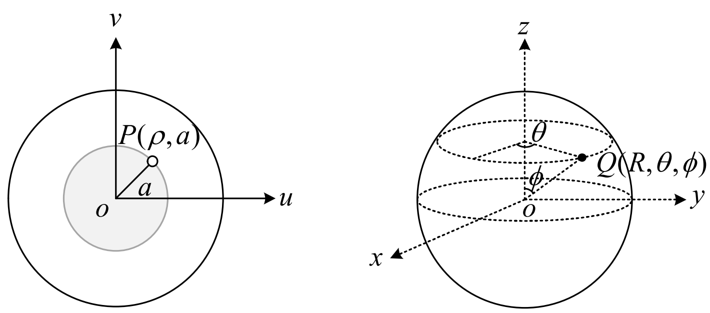

Fig. 4. Mapping diagram of S on a sphere

Let P point on the texture plane be mapped to Q points on the hemisphere, in order to effectively reduce the texture deformation, the mapping relationship between the two points is constructed by using the method of area equivalence constraint. The area equipartition constraint is to make the ratio of the area of the texture plane and the corresponding mapped area on the sphere equal to a constant K:

$$K=\frac{\pi\cdot\rho^2}{2\pi R^2(1-\cos\phi)} \tag{9}$$

Thus we get: $\rho=\sqrt{2}KR^2\left(1-\cos\phi\right)$. Let $\alpha=\theta$, the texture coordinates can be calculated as:

$$\begin{cases} u=\rho\cdot\cos\alpha=\sqrt{2KR^2\left(1-\cos\phi\right)}\cdot\cos\theta \\ v=\rho\cdot\sin\alpha=\sqrt{2KR^2\left(1-\cos\phi\right)}\cdot\sin\theta \end{cases} \tag{10}$$

When $0\le\phi\le\pi/2$, the mapping result is the upper hemisphere. When $\pi/2\le\phi\le\pi$, the mapping result is the lower hemisphere. Since the texture coordinate origin is generally located in the lower left corner, the above equation is corrected:

$$\begin{cases} u = \rho \cdot \cos\alpha = 0.5 + \sqrt{2KR^2\left(1-\cos\phi\right)} \cdot \cos\theta \\ v = \rho \cdot \sin\alpha = 0.5 + \sqrt{2KR^2\left(1-\cos\phi\right)} \cdot \sin\theta \end{cases} \tag{11}$$

By experimentation, when using a mapped texture map of size 512 × 512, take $R = 1.0, K = 0.12$.

2) O mapping: O mapping uses the third mapping method, i.e., the texture at vertex $V(x, y, z)$ on the surface of the model is taken as the ray formed by the line from the center of the object to that vertex, and the texture at the intersection with the transition surface $V'(x', y', z')$.

The shape of the model is generally more complex, and the algorithm to find the center point is as follows: Set xyz three-dimensional coordinate space, the coordinates of a vertex on the model as $P(v_x, v_y, v_z)$, calculate the sum of the values of all the vertices of the coordinate vectors, and then find out the average value of the coordinate vectors, and then get the coordinates of the center point of the object. $P'(c_x, c_y, c_z)$. The direction vector composed of the center point and a vertex is $\overrightarrow{PP} = (v_x - c_x, v_y - c_y, v_z - c_z)$, and then determine its θ and ϕ in the sphere, so as to calculate the coordinates of the center point of the object by the above formula. uv coordinates.

4. Exploration of techniques and color distribution in the creation of lacquer paintings

4.1. Exploration of color distribution based on image coloring algorithm

4.1.1. Evaluation indicators. PSNR (Peak Signal-to-Noise Ratio), SSIM (Structural Similarity), LPIPS (Learned Perceptual Image Block Similarity), and FID (Frechet Initial Distance) are used as evaluation metrics in the experiments.

PSNR, which is the peak signal-to-noise ratio, aims at comparing the absolute difference between the pixel values of the predicted image and the target image, and belongs to the evaluation metrics based on statistics, and is calculated as shown in Equation (12):

$$PSNR(x, y) = 10 \times \log_{10}\left(\frac{(MAX_l)^2}{L_2(x, y)}\right) \tag{12}$$

where, x is the predicted lacquer image, y is the target high quality image, MAX_l is the maximum pixel value of the lacquer image which is 255 in the experimental set, L_2 denotes the 2-paradigm loss, and $\log$ denotes the logarithmic computation which is used to convert the difference values to be expressed in decibels. Finally the average PSNR of the test set is taken as the final result.

SSIM is structural similarity, the goal is to compare the brightness, contrast, and structure of the predicted image with the target image, specifically, the brightness is based on the mean, the contrast is based on the standard deviation, and the structure is based on the correlation coefficient, and it is a further measure of the relative structure of the image rather than the absolute pixel difference compared to PSNR, which belongs to the evaluation index based on statistics, and the formula is shown in equation (13):

$$SSIM = \frac{\left(2\mu_x\mu_y + C_1\right)\left(2\sigma_{xy} + C_2\right)}{\left(\mu_x^2 + \mu_y^2 + C_1\right)\left(\sigma_x^2 + \sigma_y^2 + C_2\right)} \tag{13}$$

where μ_x is the mean of x, μ_y is the mean of y, σ_x^2 is the variance of x, σ_y^2 is the variance of y, and σ_{xy} is the covariance of x and y. $C_1 = (k_1 MAX_1)^2$, $C_2 = (k_2 MAX_2)^2$ are two elaborations to avoid division by zero. $k_1 = 0.03$, $k_2 = 0.09$ are the default values. i.e:

$$LPIPS(x, y) = \sum_l \frac{1}{H_l W_l} \sum_{h,w} \left\| m_l \odot \left(f_{xh,w}^l - f_{yh,w}^l \right) \right\|_2^2 \tag{14}$$

In the formula, l indicates the corresponding layer, H_l, W_l indicates the length of the height and width dimensions of the corresponding features, h, w is the serial number of traversing these two dimensions, f_x^l, f_y^l indicates the corresponding features, and m_l is used to deflate the weights of the features in the channel dimension.

FID is the Frechet initial distance, which is one of the standard indicators for evaluating the performance of generative methods today, and belongs to the evaluation indicators based on human perception, and is calculated as shown in Equation (15):

$$\begin{aligned} FID(X, Y) = {} & \left\| \mu\left(M(X) - \mu\left(M(Y)\right)\right) \right\|_2^2 + \\ & Trace\left(Cov\left(M(X)\right) + \operatorname{cov}\left(M(Y)\right) - 2\left(Cov\left(M(X)\right)\right) Cov\left(M(Y)\right)^{1/2} \right) \end{aligned} \tag{15}$$

M, μ denotes the lacquer painting image, the mean of the color distribution, Cov the covariance of the color distribution, and $Trace$ the trace of the computational matrix, respectively.

4.1.2. Results and analysis. In order for this algorithm to be effectively applied to real-world environments, two publicly available color lacquer painting datasets are used as sub-datasets in the experiments. The lacquer painting dataset containing 10,000 sheets of 1024×1024 resolution, and the lacquer painting dataset containing 20,000 sheets of 1024×1024 resolution. Combining the two corresponding different sub-datasets into an overall dataset can effectively inhibit the model from performing coloring biased towards a certain type of lacquer paintings, such as avoiding the deviation of the colors assigned to the lacquer paintings, which is an error caused by the bias of the training data. The two sub-datasets are analyzed for data distribution, and 1000 images are randomly selected from the two sub-datasets and input to the algorithm for training. The algorithm is based on NVIDIA GEFORCE GTX 4080Ti graphics card, PyTorch deep learning framework for experimentation. The grayscale paint painting data in training is input to the model for coloring prediction and parsing prediction. For model training, the batch size is 16, and the loss function is set to 0.1 to weigh the importance of the master-slave task, and 1. The coloring model and the discriminator both use the Adam optimizer, with a learning rate of 1e-3 and 1e-4, respectively. The total number of training epochs is 50, and the performance of the model is verified using a validation set for every 5 epochs, and the model with the best validation performance is used for the testing on the test set.

In the experiment, firstly, the coloring performance of different algorithms is compared, and the coloring performance comparison results are shown in Table 1. Among them, the first 2 rows show the coloring performance of two classical image translation methods, CycleGAN, Pix2Pix, and the 3rd row shows the performance evaluation of further introducing parsed images as semantic conditions in the Pix2Pix method, which is denoted as Pix2Pix-Parse. the 4th to 6th rows show the performance of the single-task ordinary convolutional model, the single-task residual structure model, and the image coloring algorithm evaluation, denoted as ST-C, ST-R, and Ours, respectively, i.e., the residual structure and face parsing tasks are gradually introduced, and PSNR, SSIM, LPIPS, and FID are adopted as the indexes for evaluating the quality of coloring. Comparing ST-R with this paper's method, it can be observed that this paper's method has a large improvement in both statistical-based and perceptual-based metrics, especially gaining 6.5 dB in PSNR and decreasing 2.9 in FID, and the same for other algorithms, which is a strong proof of the importance of this paper's method in the form of color distribution.

Table 1. Color performance comparison results

Method	PSNR ↑	SSIM ↑	LPIPS ↓	FID ↓
CycleGAN	25.28	0.858	0.146	22.27
Pix2Pix	28.47	0.948	0.066	6.56
Pix2Pix-Parse	29.76	0.956	0.058	5.57
ST-C	28.29	0.937	0.064	8.66
ST-R	28.59	0.949	0.058	7.18
MT-R-Parse	34.09	0.964	0.025	4.28

The significance of the lacquer painting color form generation task and the comparison results of the lacquer painting color form generation task are shown in Table 2. Row 1 corresponds to ST-C described above, rows 2 and 3 represent the performance evaluation of the algorithms based on the ordinary convolutional model introduced into the lacquer painting color key point detection task and the lacquer painting color resolution task, which are denoted as MT-C-Detect and MT-C-Parse, respectively, and row 4 corresponds to ST-R described above, row 5 represents the performance evaluation of the algorithm based on the residual structure model introduced into the color information key point detection task, which is denoted as MT-R-Detect, and row 6 corresponds to the algorithm of this paper. The performance of each index in the table shows that the method of this paper still performs very well in the task of color form generation of lacquer paintings, which verifies the effectiveness of the method of this paper.

Table 2. Paint color forms generate task comparison results

Method	PSNR ↑	SSIM ↑	LPIPS ↓	FID ↓
ST-C	28.29	0.939	0.064	8.66
MT-C-Detect	28.57	0.944	0.058	9.47
MT-C-Parse	31.59	0.954	0.038	6.64
ST-R	28.59	0.949	0.058	7.18
MT-R-Detect	33.36	0.956	0.029	4.86
Ours	34.09	0.964	0.025	4.28

4.2. Color Distribution and Abrasive Painting Technique Integration Analysis

4.2.1. Experimental platforms. Based on the principle of fusion of color distribution and grinding technique in lacquer painting, the experimental results were analyzed on the development platform of Visual Studio. Net 2007, using the development language of Visual C++ 7.0 (based on OpenGL graphics library), and on the operating system of WindowsXP with the configuration of Pentium V2.6GHZ, 512M DDR RAM, Intel 82865G graphics controller, and Windows XP operating system. WindowsXP operating system to analyze the experimental results.

4.2.2. Simulation analysis. This chapter first demonstrates and analyzes the rendering effects of the color distribution of lacquer paintings and the glory deterioration of the abrasion painting technique for each simulation target, then analyzes the efficiency of their operation, and finally gives a series of comprehensive effect diagrams.

The efficiency of the whole simulation process depends on the following factors: the running environment of the system, the efficiency of the development language, the efficiency of the program design, the complexity of the input model (mainly referring to the number of facets, disregarding the model of the object with complex construction. There is also the length of the sketch lines, the size of the 2D projection area, etc.), the simulation efficiency by a large extent depends on the efficiency of the algorithms, so the analysis of the efficiency of the whole system operation here also represents only the efficiency of the rendering system based on this particular pen model. In addition, the configuration environment used for the experiment has been described at the beginning of this section, so the simulation efficiency in this paper is mainly determined by the data complexity. When the number of mesh facets = 6500, the corresponding 3D mountain stone mesh is shown in Fig. 5. Fig. 6 and Fig. 7 respectively give the effect of generating the contour lines of the mountain stone and the mountain stone grinding technique under the premise of inputting this graphic, and finally the rendering of these paintings after loading the texture, and the fusion effect of the contour lines and the mountain stone grinding technique is shown in Fig. 8. The experimental data of the fusion of contour line and stone grinding technique is shown in Table 3. From the careful analysis of the experimental data, it is easy to see that: first of all, the number of faces is the dominant factor affecting the efficiency of the experiment for a certain level of algorithmic efficiency, and with the increase of the number of faces, the construction time of the 3D rocks, the finding time of the rock contour lines, and the incorporation time of the grinding and painting technique will be increased at the same time. Secondly, the length of the frontal sketch curve and the length of the bottom sketch curve entered by the user do not have a great influence on the simulation efficiency. Finally, the simulation effect can achieve a certain degree of real-time. From the careful analysis of the experimental data, it is not difficult to see that: firstly, under a certain efficiency of the algorithm, the number of faces is the dominant factor affecting the efficiency of the experiment, and with the increase of the number of faces, the construction time, the finding time of the outline lines of the rocks, and the fusion time will increase at the same time. Secondly, the length of frontal sketch curve and the length of bottom sketch curve inputted by the user do not have a great influence on the simulation efficiency. Finally, the simulation effect can achieve a certain degree of real-time.

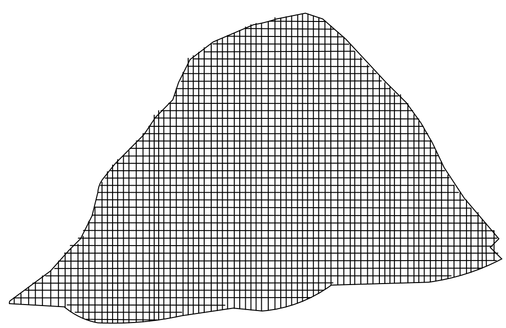

Fig. 5. Corresponding 3d mountain grid

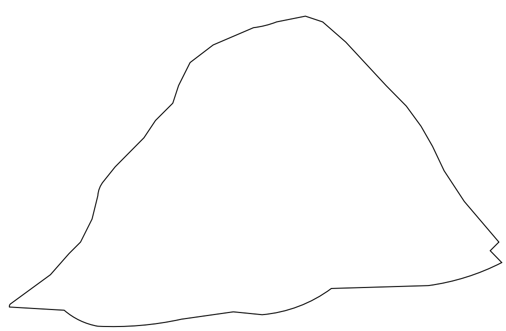

Fig. 6. Find the outline of the rock

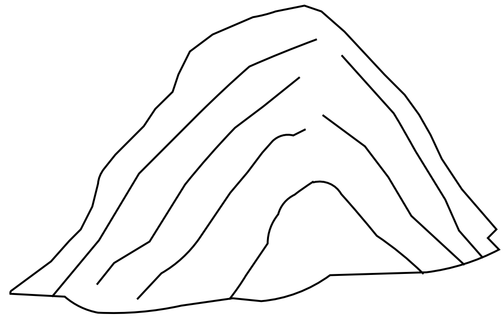

Fig. 7. Renderings of stone grinding techniques

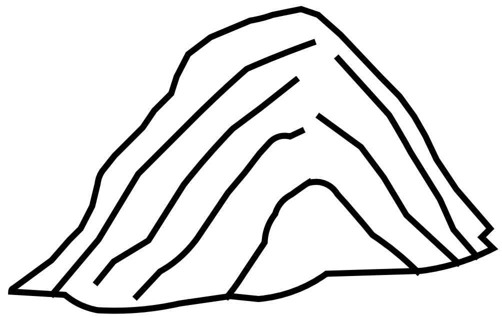

Fig. 8. The fusion effect of contour line and mountain stone grinding technique

Table 3. Experimental data

Complexity			Build time(ms)	Search time(ms)	Fusion time(ms)	Total render time(ms)
Sketch curve length on front(cm)	The length of the outline curve is (cm)	Number of pieces				
30.841898	64.499398	600	1675	2900	21500	36800
25.751213	63.707943	2600	3048	7100	29800	49100
24.834823	63.995361	6600	3300	9600	32300	56500
24.92654	65.126727	12400	3500	12000	38700	60800

In this environment, we conducted the experiments in this paper using different models. The experiments conducted in this paper are drawn in a window of size 256×256 and the rendering efficiency is shown in Table 4. To perform distance-based LOD selection requires the computation of the two drawing methods, which requires interpolation, and since interpolation requires only one step of operation, for a model with multiple facets, its computation is approximately equal to the sum of the computation of the two drawing techniques. According to the degree of fluency required by the naked eye, we know that generally 0~90FPS can be called real-time. Therefore, the rendering method proposed in this paper meets the requirements of real-time drawing, which can be applied to the fusion of grinding drawing techniques and color distribution in the creation of lacquer paintings, and is of great significance to the digital inheritance and development of lacquer paintings.

Table 4. Rendering efficiency

Model	Model	Rendering Mode (FPS)		
		Contour internal integration	Single stroke rendering	Ours
1	4160	116	84	86
2	1154	126	96	81
3	6132	87	64	77
4	16059	68	49	59
5	18314	59	43	42

5. Conclusion and outlook

5.1. Conclusion

Combined with the characteristics of the abrasive painting technique, the aesthetic performance of the abrasive painting technique in terms of color language is described. In order to realize the mutual integration of the abrasive painting technique and the form of color distribution, the image coloring algorithm is adopted to generate the color distribution information of lacquer paintings, and then the texture mapping operation of the renderer is used to promote the mutual integration of lacquer paintings' colors and the abrasive painting technique. Finally, comprehensive evaluation indexes and experimental platforms are used to analyze the abrasive painting technique and color distribution in lacquer painting transmission. In the comparison of coloring performance, the four index values of this paper's method are 34.09, 0.964, 0.025, and 4.28, which all outperform other methods, and there is a type of phenomenon in the generation of lacquer painting color forms. Setting the algorithm efficiency for a fixed value, the number of face pieces of lacquer painting images, the contour line finding time of the image, the integration of color and grinding painting techniques show a growing trend, and its simulation effect can meet the needs of the combination of grinding painting techniques and algorithm-generated color distribution methods, and better promote the inheritance of lacquer painting creation.

5.2. Outlook

Lacquer painting has developed to date with numerous techniques. The research on the lacquer painting technique in this paper provides some new thinking and innovative points to a certain extent. However, there are still many shortcomings, such as the experimental part of the work on the writing performance of the grinding and painting technique is still lacking and not deep enough. As well as the research content is relatively single, not rich enough. Therefore, for the subsequent research, we will continue to dig deeper into the “writability” of the mill-painting technique, and we will also try to combine the color attributes with other techniques to enrich the effect of the picture, and at the same time, we will continue to explore the possibilities of more expressions of the mill-painting technique.

References

[1] Ye, Z., & Jiao, X. (2022). Contemporary art on realistic subjects in the new era of lacquer painting. Asian Journal of Social Science Studies, 7(7), 75.

[2] Jin, Y. (2024). Research on the Application of Lacquer Painting Techniques in Modern Handicrafts. Frontiers in Art Research, 6(9).

[3] Lin, Z. (2020, September). Inheritance and Transmutation: Discussion on the Artistic Features of Chinese Lacquer Painting. In 4th International Conference on Art Studies: Science, Experience, Education (ICASSEE 2020) (pp. 607-612). Atlantis Press.

[4] Abdel-Ghani, M. (2022). Multidisciplinary study of a Qajar lacquered painting: Technology and materials characterization. Vibrational Spectroscopy, 119, 103355.

[5] Chang, B. (2020). Traditional Technique of Lacquer. In Thirty Great Inventions of China: From Millet Agriculture to Artemisinin (pp. 313-342). Singapore: Springer Nature Singapore.

[6] Zhao, F., Sun, M., Tie, F., Wu, C., Zhang, X., & Mu, X. (2020). Inlaid materials and techniques of an ancient Chinese bronze mirror. The European Physical Journal Plus, 135(8), 666.

[7] Shahriar, S. (2022). GAN computers generate arts? A survey on visual arts, music, and literary text generation using generative adversarial network. Displays, 73, 102237.

[8] Li, M., Lv, J., Wang, J., & Sang, Y. (2020). An abstract painting generation method based on deep generative model. Neural Processing Letters, 52, 949-960.

[9] Ji, S., Yang, X., & Luo, J. (2023). A survey on deep learning for symbolic music generation: Representations, algorithms, evaluations, and challenges. ACM Computing Surveys, 56(1), 1-39.

[10] Kang, Y., & Kim, J. (2024). Animation Character Generation and Optimization Algorithm Based on Computer Aided Design and Virtual Reality. Computer-Aided Design and Applications, 21(S14), 46-62.

[11] Elstermann, A. (2020). Computer-generated text as a Posthuman mode of literature production. Open Library of Humanities, 6(2).

[12] Ranjan, R., Mishra, A., Maharana, S. P., & Kumari, S. (2024). AI in Visual Arts: Exploring Generative Algorithm. In The Pioneering Applications of Generative AI (pp. 41-60). IGI Global.

[13] Chen, H. (2024). Painting Style Conversion and Artistic Creation Exploration Based on Deep Learning. International Journal of High Speed Electronics and Systems, 2540168.

[14] Xu, X. (2024). A fuzzy control algorithm based on artificial intelligence for the fusion of traditional Chinese painting and AI painting. Scientific reports, 14(1), 17846.

[15] Yan Du. (2024). Exploring the Transmission of Chinese Classic Culture in the Western World Based on the English Translation of Tao Te Ching. Journal of Humanities, Arts and Social Science(10).

[16] Zixian Ye. (2024). Intralingual and Interlingual Translation of Chinese Classics—Taking the English Translation of the Tao Te Ching as an Example. English Language Teaching and Linguistics Studies(5).

[17] Yuwei Feng & Feng Shi. (2024). The Application of Lacquer Painting in Public Art: An Analysis from the Perspective of Vocational Education. Urban Design(2),

[18] Yipin Chen. (2023). The visual beauty of modern lacquer painting colors. Frontiers in Art Research(16).